Formation Regularities of Gaseous Vapour Plasma Envelope in Electrolyzer

S. Yu. Shadrin, A. V. Zhirov, P. N. Belkin

Nekrasov Kostroma State University,
1 May, str., 14, Kostroma, 156961, Russia, e-mail: syushadrin@yandex.ru

This work focuses on the factors causing appearance of a steady and continuous vapour-gas envelope which functions as medium for plasma electrolytic saturation of metal and alloys with interstitial elements (nitrogen, carbon, and boron). It is established that second critical voltage associated with transition from the current oscillation mode to the stable heating is determined by anion emission from boiling electrolyte in the envelope and heat transfer conditions in the system. Stability of the interface electrolyte–envelope is provided by the energy liberation in the envelope due to the passage of current. Second critical voltage promoting the anion emission is calculated on the base of Gouy–Chapman model and Tonks–Frenkel aperiodic instability. Theoretical dependence of critical voltage on the electrolyte concentration is confirmed experimentally. The influence of the electrolyte concentration on the second critical voltage is explained by the ability of the electrolyte to emit anions. Effect of solution flow rate on this voltage accounts for heat transfer conditions. It should be noted that the anion emission explains the influence of electrolyte composition on the weight change of the anode sample, limit heating temperature (~1000°C) due to the limited emissivity of electrolyte, discrete current in the case of a small surface anode, and high-frequency pulse of the current.

Keywords: plasma electrolysis, anions emission, critical voltage.

УДК 621.785.53; 621 3.035.183

INTRODUCTION

Plasma electrolytic treatment (PET) claims the increasing attention of researchers as a rapidly developing area of surface engineering owing to new opportunities of its various applications [1–3]. These applications include cleaning processes of steel surface [4]; the methods of steel hardening [5] and rapid surface annealing of peened steel [6]. Saturation processes include nitriding of the cast iron and cast steel [7], carbonitriding of steels [8–11], carburizing [12, 13], boronizing [14] and borocarburizing [15]. Pulse plasma electrolytic saturation (PES) is particularly significant because this method makes it possible to form the nanostructured layers with advantageous properties [16, 17]. As a rule, PES is realized at voltages enabling the appearance of three-phase systems (i.e. metal – vapour-gas envelope (VGE) – electrolyte) disregarding a possible oxide layer on the electrode surface [1]. Those systems differ in types of electrical discharges, chemical and electrochemical reactions, etc. The electrode is surrounded by the continuous or discontinuous, steady or unsteady electrically conductive VGE. The continuous and unsteady VGE formed at voltage higher than critical U_1 is condensed periodically and formed again [1, Figure 2a]. The value U_1 determines the energy required for the electrolyte vaporization around workpieces [18].

Steady and continuous VGE is formed when voltage goes up to U_2. This state is similar to film boiling but differs from it by the presence of internal heat sources in the VGE. The steady and continuous VGE exists only when the value of the heat flux from the VGE to electrolyte exceeds the critical flux q_{min} enabling the film boiling [19]. This heat flux can arise only owing to the sufficient energy release in the VGE due to the current passing through it. Thus, the key issue of the stationary PES existence is a proper conductivity of the VGE which depends on the active electrode polarity. Electrical discharges are assumed to provide VGE conductivity, if the active metallic electrode is a cathode capable of providing intense electron emission. It is established that the emission spectrum of the cathode VGE contains the lines of the system elements [20].

Conversely, ionization of the anode VGE in the voltage interval from 100 to 300 V is not found, and the glow spectrum is characteristic to that of a heated body [18]. In this case, the electrolyte surface near the VGE is a cathode where the electron emission is at least problematic. We assume (as in our earlier work) that the base charge transfer through the anode VGE at voltages up to 250–300 V occurs via anion emission and their transition from boiling electrolyte to anode under electric field [21]. This paper focuses on the theoretical analysis of anion transfer from electrolyte to the VGE and confirmation of this mechanism by the experimental study of influence of the treatment conditions on the second critical voltage.

EXCESS CHARGE EVALUATION IN THE SURFACE LAYER OF AQUEOUS ELECTROLYTE

The simplest variant of the anode PES for the steady-state system within the range from 100 to 300 V is considered [3]. Appropriate thermal models for calculation of the anode temperature, current density, and the VGE thickness are developed [22]. The heat evolving in the VGE transfers to the anode, electrolyte, and atmosphere. The electrolyte temperature distribution is supposed to be constant. The electrolyte temperature at the VGE–electrolyte boundary is 100°C; it decreases to normal room temperature at a longer distance from VGE. This state is provided by electrolyte cooling with the use of heat exchanger.

Consider the state of the electrolyte near the VGE. The aqueous electrolyte surface contains ions and molecules of the solved substances; water molecules partly belong to solvated ions. Some ions can be transferred from the electrolyte to the VGE during the process of boiling because of the interaction with water molecules. The ions are not able to move over a long distance from the solution because of the electrical forces which are associated with the uncompensated charge of the ions remaining in the electrolyte However, some of emitted ions do not return to solution even if the electric field is available. In this case the solution surface will get the negative charge owing to the increased anion concentration (Figure 1).

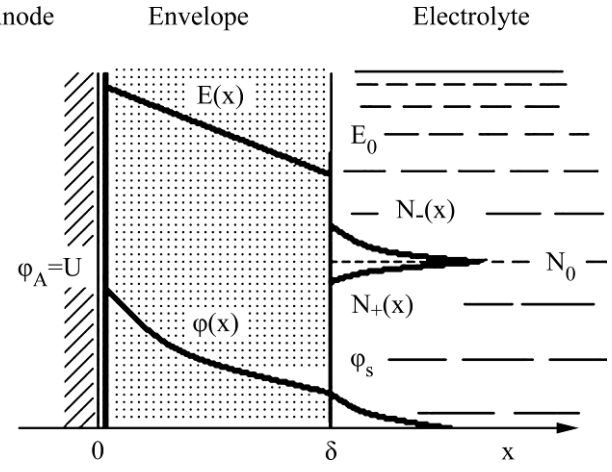

Fig. 1. Potential distribution in the system under consideration.

It should be noted that in the case of double layer existing on the interface without the external electric field is not considered here. An excess surface charge can be evaluated by Gouy–Chapman model where the ions concentration is described by Boltzmann distribution law.

In practice, the anode surface area must be at least an order of magnitude smaller than that of the cathode. For this reason, the maximal current density and Joule heat evolution are observed at the anode. Lines of current have axial symmetry in the cylindrical work chamber; electric field distribution may be more complex in other cambers. However, we can ignore these effects near the anode as the VGE thickness is by a factor of tens smaller than the anode size. This fact enables us to use a single-dimensional case with coordinate directed perpendicular to the anode surface.

Let us denote the electrostatic potential in the VGE and the solution $\varphi(x)$ where axis x is perpendicular to the interface. Let us also denote the bulk concentration ions N_0, then the concentrations of the ions of any species in the electrolyte is

$$N_+ = N_0 \exp\left[-\frac{e\varphi(x)}{kT}\right] \text{ and } N_- = N_0 \exp\left[\frac{e\varphi(x)}{kT}\right], \quad (1)$$

where e is the elementary charge, k is the Boltzmann constant, T = 373K is the boiling solution temperature.

The excess charge per unit volume in the surface layer is then

$$\rho_e(x) = e\left[N_+(x) - N_-(x)\right] = -2eN_0 \operatorname{sh}\left(\frac{e\varphi(x)}{kT}\right). \quad (2)$$

Potential distribution in the electrolyte is described by the Poisson equation:

$$\frac{d^2\varphi(x)}{dx^2} = -\frac{\rho_e(x)}{\varepsilon\varepsilon_0} = \frac{2eN_0}{\varepsilon\varepsilon_0} \operatorname{sh}\frac{e\varphi(x)}{kT}, \quad (3)$$

where ε is the dielectric constant of the solution, $\varepsilon_0 = 0.885 \cdot 10^{-11}$ F/m is electric constant.

The electric field strength is recognized to be zero at distances far from the VGE then integration gives:

$$\frac{d\varphi}{dx} = -\sqrt{\frac{4kTN_0}{\varepsilon\varepsilon_0}\left[\operatorname{ch}\frac{e\varphi(x)}{kT} - 1\right]} \text{ or}$$

$$\frac{d\varphi}{dx} = -\sqrt{\frac{8kTN_0}{\varepsilon\varepsilon_0}} \operatorname{sh}\frac{e\varphi(x)}{2kT}. \quad (4)$$

Second integration leads to potential of the excess charge in the electrolyte

$$\varphi(x) = \frac{4kT}{e} \operatorname{arth}\left[C\exp(-\alpha x)\right];$$

$$C = \operatorname{th}\frac{e\varphi_s}{4kT} \quad \alpha = e\sqrt{\frac{2N_0}{\varepsilon\varepsilon_0 kT}}, \quad (5)$$

where $\varphi_s = \varphi(\delta)$ is the surface solution potential. Constant C may be determined through the electric field strength at the VGE boundary:

$$E(x) = -\frac{d\varphi}{dx} = \sqrt{\frac{8kTN_0}{\varepsilon\varepsilon_0}} \operatorname{sh}\left[2\operatorname{arth} C\exp(-\alpha x)\right] = \quad (6)$$

$$= \sqrt{\frac{8kTN_0}{\varepsilon\varepsilon_0}} \frac{2C\exp(-\alpha x)}{1 - C^2\exp(-2\alpha x)}.$$

It is obvious that $E_v = \varepsilon E(0)$ at the envelope–electrolyte boundary where E_v is the electric field strength at this boundary and $\varepsilon \approx 1$. Then

$$E(0) = \frac{E_v}{\varepsilon} = \sqrt{\frac{8kTN_0}{\varepsilon\varepsilon_0}}\frac{2C}{1-C^2}. \quad (7)$$

The electric field strength in the VGE does not exceed the breakdown field strength at the atmospheric pressure therefore we suppose that $E_v = 10^6$ V/m. Constant C is found by solving Eq. (7) with the use of the following parameters: $k = 1.38\cdot10^{-23}$ J/K; $T = 373$K; $N_0 = 6\cdot10^{26}$ m^{-3} (1M aqueous solution NH_4NO_3); $\varepsilon = 81$. According to our estimates $C = 3.32\cdot10^{-5} << 1$ that allows us to simplify the formula (5) and (6):

$$\varphi(x) = \frac{4kT}{e}C\exp(-\alpha x) = \varphi_s\exp(-\alpha x), \text{ and}$$

$$E(x) = 4\sqrt{\frac{2kTN_0}{\varepsilon\varepsilon_0}}C\exp(-\alpha x). \quad (8)$$

Value C can be determined as follows. Electrolyte surface instability may contribute to field and thermal evaporation of the anions [23]. It is shown theoretically that vapor circulation in VGE along the electrolyte surface may generate Kelvin–Helmholtz oscillatory instability. Furthermore, the electrolyte–VGE interface has a high charge density which may cause the Tonks–Frenkel aperiodic instability of the electrolyte surface at sufficient voltage. The electric field strength in the VGE provided for the anions emission from the boiling electrolyte to the VGE is reached at the critical surface charge density of the electrolyte surface [24]:

$$q_{e0} = \sqrt[4]{4g\sigma\rho\varepsilon_0^{\,2}}, \quad (9)$$

where g is acceleration due to gravity, σ is surface tension coefficient of the electrolyte, ρ is its density.

The critical charge corresponds to the critical electric field strength in the plane VGE near the electrolyte surface:

$$E_{cr} = \frac{q_{e0}}{\varepsilon_0} = \frac{\sqrt[4]{g\sigma\rho\varepsilon_0^2}}{\varepsilon_0}. \quad (10)$$

Then, we can find C, using (8) and the relation between the field strengths and the interface:

$$E(0) = \frac{E_{cr}}{\varepsilon} = 4\sqrt{\frac{2kTN_0}{\varepsilon\varepsilon_0}}C = \frac{\sqrt[4]{g\sigma\rho\varepsilon_0^2}}{\varepsilon\varepsilon_0} \text{ and}$$

$$C = \frac{\sqrt[4]{g\sigma\rho}}{4\sqrt{2\varepsilon kTN_0}}, \quad \varphi_s = \frac{\sqrt[4]{g\sigma\rho}}{e}\sqrt{\frac{kT}{2\varepsilon N_0}}. \quad (11)$$

The excess of U_2 corresponding to E_{cr} results in the instability of the electrolyte surface with ejection of the excess charge in the VGE. Negative ions emitted to the VGE drift in the direction of the anode with the energy dissipation that provides the VGE heating. The surface electrolyte potential is suggested to be proportional to the applied voltage with factor b thus we obtain the dependence of U_2 on the electrolyte concentration:

$$U_2 = \frac{b}{e}\sqrt[4]{g\sigma\rho}\sqrt{\frac{kT}{2\varepsilon N_0}}. \quad (12)$$

The decreasing dependence of U_2 on the electrolyte ions concentration has been obtained experimentally (Fig. 2) in our earlier work [25].

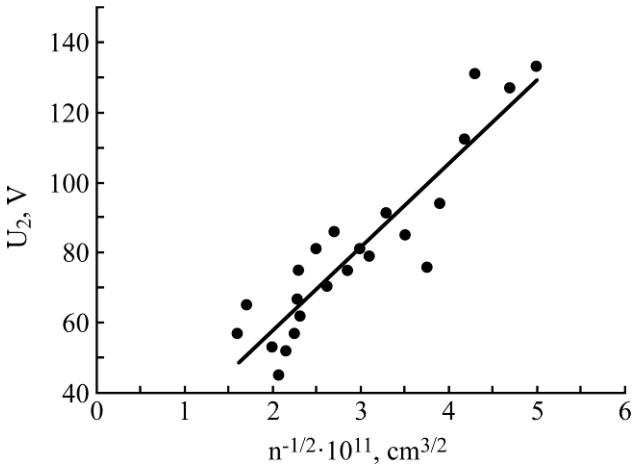

Fig. 2. Dependence of voltage U_2 on volume ion concentration NO_3^- of ammonium nitrate solution [26].

EXPERIMENTAL

Measurements were carried out using an electrolyte plasma treatment unit. The sample was treated under the conditions of electrolytic longitudinal flow in an electrolyser – a cylindrical stainless steel vessel of 100 mm in its inner diameter and 210 mm high (Figure 3). Electrolyte circulation is realized by a pump UntiStar POW–300 4L. The electrolyte is cooled in a heat exchanger by tap water; electrolyte temperature is stabilized at 15–16°C. Electrolyte flow rate is measured by a flowmeter RMF-0.16 GUZ (accuracy to within ±2.5%) and ranged from 0 to 3 l/min.

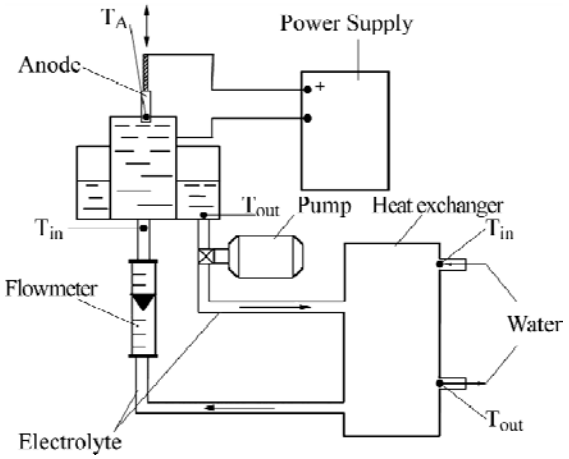

Fig. 3. Schematic illustration of coating setup.

An aqueous solution containing ammonia nitrate was chosen as electrolyte; its concentration (1–3 mol/l) is controlled by measuring density. This composition is characterized by high conductivity and small anode dissolution of the steel workpieces.

All measurements are carried out with the use of cylindrical workpieces of medium-carbon steel 45 (0.45% C) with a diameter from 7.4 to 22 mm and 250 mm in length (Figure 4). The appearance and state of the VGE are studied on the exposed part of workpieces with height 2 mm submerged at a depth of 50 mm. The remaining surface of a sample is covered by insulating tape.

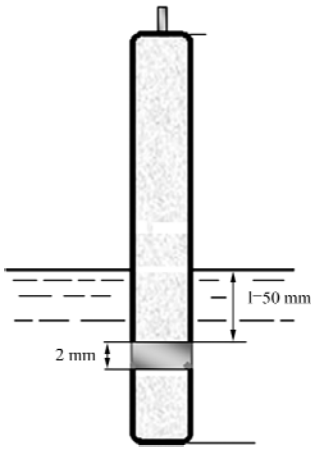

Fig. 4. Sample-anode.

The critical voltage U_2 is found as follows. An anodic sample is submerged into the flowing electrolyte. Then the sample is voltage biased with a positive value. Electric current in the VGE and its frequency spectrum are recorded with an oscillograph Zet 302 during 60 s. The measurements are repeated with increasing voltage from 60 V up, by 1 V at a time. The current oscillation mode always occurs at the beginning of the measurement, its average value exceeding 10 A. It is accepted that U_2 is a minimal voltage which provides current oscillation disappearance sooner than after 60 s and the VGE appearance fixed by a sharp decrease in current. Two measurements are given here as examples. In the first case, the voltage on the power supply is 68 V at an open circuit. This voltage is decreased to 46.4 V after closing the circuit, current oscillates from 8.72 to 9.36 A. The VGE appearance is not detected during 60 s. In the second case, the voltage 69 V at an open circuit decreases to 49 V after closing it and current oscillates in the range 9.04–9.72 A. After 46.3 s the current is decreased to 0.96 A owing to the VGE appearance and the voltage reaches 68.6 V. Hence, the value of the second critical voltage is 69 V under these conditions.

The voltage is measured with the voltmeter LM-1 (accuracy to within ±0.5%). The value of current is fixed with the use of digital multimeters MY–64 and MS 2101 (accuracy to within ±0.5%). The electrolyte temperature is measured with a digital thermometer MS-6501 with a thermocouple (accuracy to within ±3%).

RESULTS AND DISCUSSION

Figure 5 shows the current oscillogram and spectrum associated with the current oscillation mode with peculiar pulses and a relatively wide frequency range. It is essential that the current drops to zero, hence the VGE loses its conductivity for a short period and gets condensed, thereafter, and this process is repeated.

Another oscillogram is observed in the mode of stationary anode heating when the VGE is steady and continuous (Figure 6). The pulse of current never drops to zero in this case. An average current magnitude is much less in comparison with that observed at the conventional electrolysis because of the envelope with higher electrical resistance appearance.

Figure 7 shows the dependence of the critical voltage U_2 on the electrolyte concentration which corresponds to the formula (12). A higher concentration of ions in the electrolyte bulk results in their higher concentration in the surface layer with the excess charge. Consequently, a smaller voltage of the external field is required for their extraction from the electrolyte. Therefore, the electrolyte with the higher ions concentration seems to have a higher emission ability.

Voltage U_2 is established to depend on the electrolyte flow velocity. Values of U_2 are presented in Fig. 8 including the case of the condition of natural convection. These increasing dependences of U_2 on the Q can be accounted for the effect of two processes. The first one is associated with an additional solution movement in the case of the forced electrolyte flow which promotes its stirring and inhibits to the directed charges migration under an electric field, that is, towards the VGE. The second process may be related to the heat transfer in the studied system. The higher the electrolyte flow velocity is, the higher is the required heat flux from the VGE to the electrolyte. This means that the emission ability of the electrolyte fixed at this constant concentration is not the only key parameter of the system. The critical voltage U_2 appropriated to the unmoved electrolyte does not provide the existence of a continuous and steady VGE if the electrolyte moves. Additional energy required for the VGE existence is provided by means of increasing U_2. Figure 9 demonstrates the dependence of U_2 on the anode diameter.

The U_2 values increase with the increase in the sample diameter. This dependence is interpreted by the heat transfer features in the studied three-phase

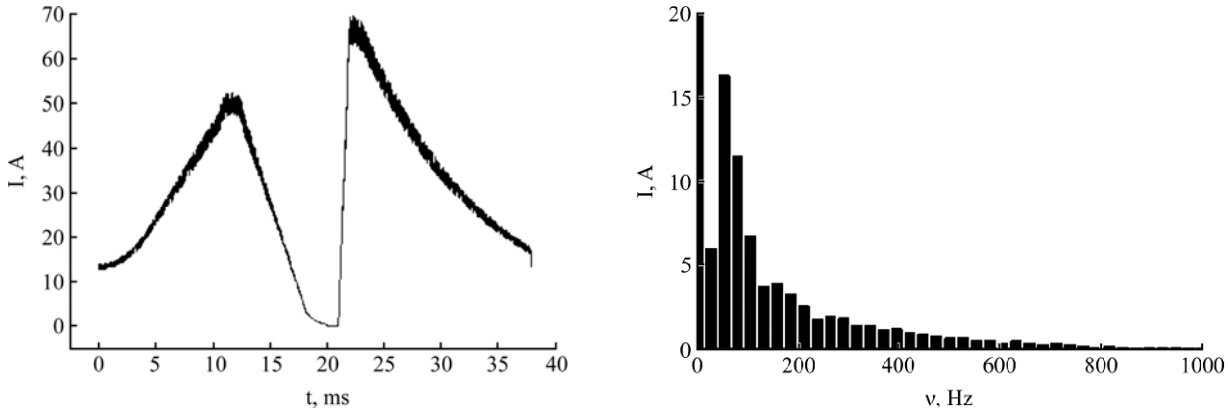

(a) (b)

Fig. 5. Current oscillogram (a) and current spectrum (b) in the oscillation mode. Voltage 60 V, NH_4NO_3 concentration 2 mol/l, sample diameter 12 mm.

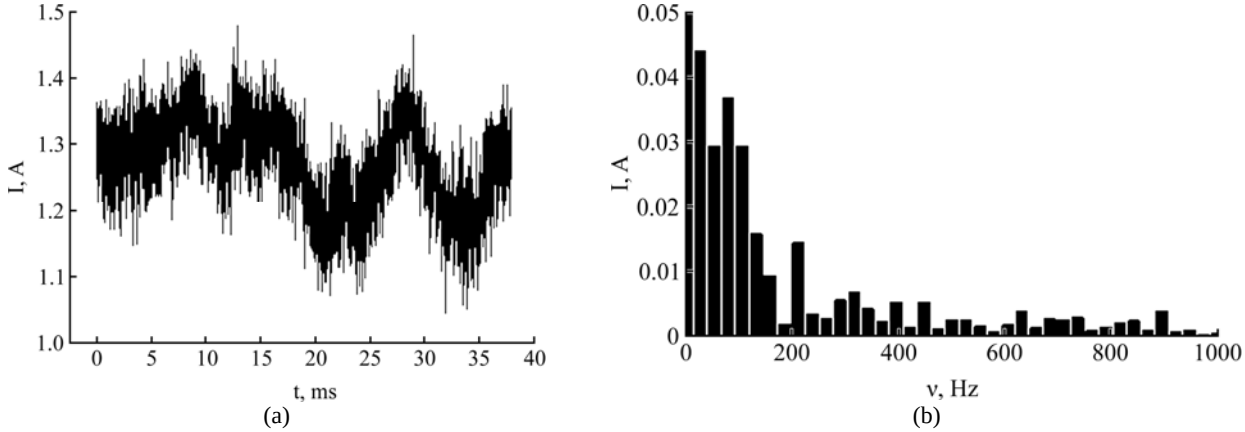

(a) (b)

Fig. 6. Current oscillogram (a) and current spectrum (b) in the anode stationary heating. Voltage 200 V, NH_4NO_3 concentration 2 mol/l, sample diameter 12 mm.

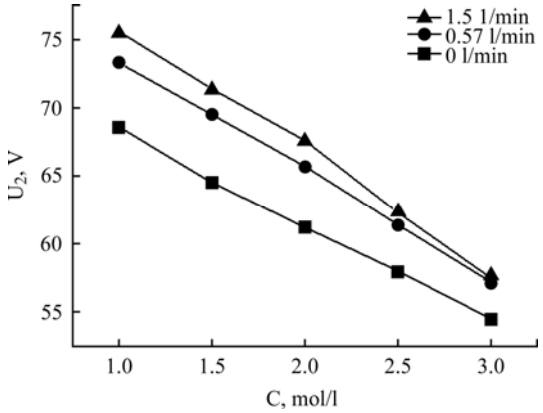

Fig. 7. Critical voltage U_2 dependence on the solution concentration over various electrolyte flow rates. Sample diameter is 12 mm.

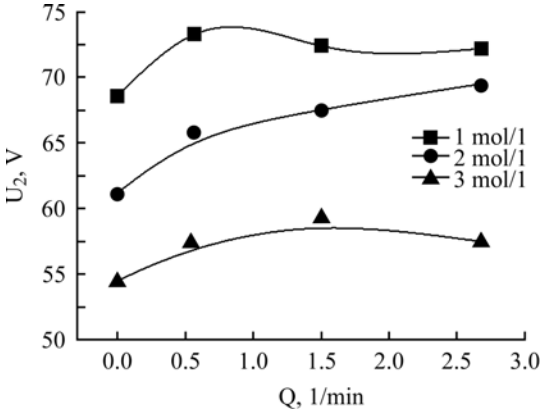

Fig. 8. Critical voltage U_2 dependence on electrolyte flow rate for various NH_4NO_3 concentrations. Sample diameter is 12 mm.

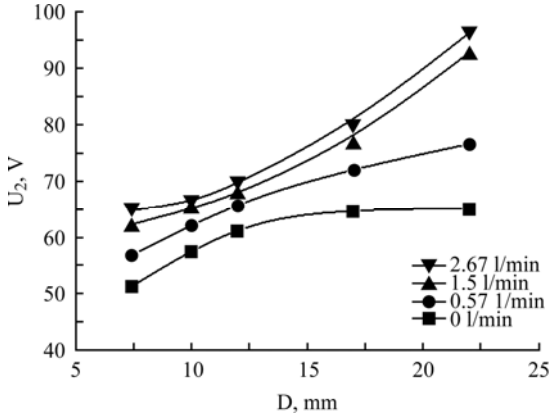

Fig. 9. Critical voltage U_2 dependence on the sample diameter over various electrolyte volume flow rates. NH_4NO_3 concentration is 2 mol/l.

system (metal–gas–electrolyte). Voltage determines the power generated in the VGE, it is partly transferred into the electrolyte and provides the steady VGE–electrolyte interface. The heat flux from the VGE to the electrolyte is proportional to the VGE area, that is, to the diameter of the sample. The heat transferred from the VGE through the sample cross-section comes to its part protruding over the electrolyte surface and further into the atmosphere by convection. This heat part is proportional to the cross-sectional area of the sample, i.e. to its squared diameter. Therefore, the heat transfer from VGE to the sample with its diameter increases more rapidly than the heat flux to the electrolyte. Hence, the minimum heat flux $q_{\min}$ from the VGE to the electrolyte may be provided by the increase in voltage when the sample diameter is increased.

CONCLUSIONS

Anode PES of metals and alloys with the interstitial elements (nitrogen, carbon, boron) was carried out under the conditions of workpiece stationary heating. This state can be realized only in the case of the steady and continuous VGE thus preventing from any contact between the electrolyte and the workpiece. The basic condition of VGE is a sufficient heat flux from the VGE to the electrolyte (at least the critical heat flux). Meanwhile, a heat flux to electrolyte is associated with the energy magnitude generated in the VGE which is dependent on the electrical conductivity of the vapour-gas media. Consequently, the critical voltage U_2 corresponding to transition from the current oscillation mode to the stationary heating is associated not only with the heat liberation providing electrolyte boiling but also with the critical field strength in the VGE which is capable of producing its conductivity. The known concept of anion emission explains virtually all experimental data. These include the influence of the electrolyte composition on the anode mass change (anode dissolution and oxidation) [3, 26], a limit heating temperature (~ 1000°C) due to the limited emissivity of electrolyte [21], a discrete current in the case of a small surface anode, and high-frequency pulse of the current [21]. It should be noted that deposition of the solution components (for example, sodium chloride or sodium carbonate) is observed on the anode surface or the chamber walls near the processing zone [18]. The ions of any species transfer to the VGE but negative ones dominate affecting the charge transfer and electrochemical reactions on the anode surface. Other ions entering the atmosphere recombine and are deposited on the surfaces with a sufficiently low temperature. This fact limits the kinds of substances in the solutions; the components with low sublimation temperature (up to 400°C) are useful only for the anode PES. For this reason the ammonium salts are often used in the electrolytes for PES. These salts do not form a layer on the anode nor sediment on the unit parts distant from the heating zone.

Factual findings are as follows:

1. The method of calculation of the second critical voltage U_2 on the base of the Gouy–Chapman model and Tonks–Frenkel aperiodic instability of the electrolyte surface under electrical field is proposed. Calculation results explain the decreasing dependence of the U_2 on the electrolyte concentration and its increasing dependence on the electrolyte temperature according to formula (12).

2. Values of the second critical voltage and the critical heat flux generated in the anode region and associated with U_2 are measured. It is established that both values are increased with the electrolyte flow rate. Heat transfer from the envelope to the electrolyte is carried out through its boundary layer; the thickness of this layer is decreased with the increase in the electrolyte flow rate. Hence, the temperature gradient, the heat flux density q_2, and the critical voltage U_2 are increased. In addition, the regularities of heat transfer permit us to explain the increase in critical voltage with the increase in the diameter of the sample-anode.

ACKNOWLEDGMENTS

This work was supported by the research program of the Ministry of Education and Science of the Russian Federation (Contract No. 855). This research was financially supported by the Russian Science Foundation (Contracts No. 15-13-10018) (experimental part "Experimental") and Contracts No.15–19–20027 (theoretical part "Excess Charge Evaluation...") to the Nekrasov Kostroma State University.

REFERENCES

1. Yerokhin A.L., Nie X., Leyland A., Matthews A., Dowey S.J. Plasma Electrolysis for Surface Engineering. *Surf Coat Tech.* 1999, **122**, 73–93.
2. Gupta P., Tenhundfeld G., Daigle E.O., Ryabkov D. Electrolytic Plasma Technology: Science and Engineering. An Overview. *Surf Coat Tech.* 2007, **201**(21), 8746–8760.
3. Belkin P.N. Anode Electrochemical Thermal Modification of Metals and Alloys. *Surf Eng Appl Electrochem.* 2010, **46**(6), 558–569.
4. Meletis E.I., Nie X., Wang F.L., Jiang J.C. Electrolytic Plasma Processing for Cleaning and Metal-coating of Steel Surface. *Surf Coat Tech.* 2002, **150**, 246–256.
5. Pat. 6,022,468 USA (C21D 1/00) Electrolytic Hardening Process / Luk S.–F., Leung T.–P. Miu W.–S., Pashby I.–R. 08.02.2000.

6. Liang J., Wang K.Y., Guo S.M., Wahab M.A. Influence of Electrolytic Plasma Process on Corrosion Property of Peened 304 Austenitic Stainless Steel. *Mater Lett*. 2011, **65**, 510–513.

7. Nie X., Wang L., Yao Z.C., Zhang L., Cheng F. Sliding Wear Behaviour of Electrolytic Plasma Nitrided Cast Iron and Steel. *Surf Coat Tech.* 2005, **200**-(5–6), 1745–1750.

8. Shen D.J., Wang Y.L., Nash P., Xing G.Z. A Novel Method of Surface Modification for Steel by Plasma Electrolysis Carbonitriding. *Mat Sci Eng A Struct*. 2007, **458**, 240–243.

9. Taheri P., Dehghanian Ch. A Phenomenological Model of Nanocrystalline Coating Production using Plasma Electrolytic Saturation (PES) Technique. *Trans B: Mech Eng.* 2009, **16**(1), 87–91.

10. Pang H., Zhang G.-L., Wang X.-Q., Lv Guo-Hua, Chen Huan, Yang Si-Ze. Mechanical Performances of Carbonitriding Films on Cast Iron by Plasma Electrolytic Carbonitriding. *Chinese Phys Lett.* 2011, **28**(11), 103–118.

11. Belkin P., Kusmanov S., Naumov A., Parkaeva Yu. Anodic Plasma Electrolytic Nitrocarburizing of Low-carbon Steel. *Adv Mater Res.* 2013, **704**, 31–36.

12. Tarakci M., Korkmaz K., Gencer Y., Usta M. Plasma Electrolytic Surface Carburized and Hardening of Pure Iron. *Surf Coat Tech.* 2005, **199**(2–3), 205–212.

13. Belkin P.N., Dyakov I.G., Zhirov A.V., Kusmanov S.A. and Mukhacheva T.L. Effect of Compositions of Active Electrolytes on Properties of Anodic Carburization. *Prot Met Phys Chem Surf.* 2010, **46**(6), 715–720.

14. Bejar M.A., Henriquez R. Surface hardening of Steel by Plasma-electrolysis Boronizing. *Mater Design* 2009, **30**, 1726–1728.

15. Wang B., Xue W., Wua J., Jin X., Hua M., Z. Wu J. Characterization of Surface Hardened Layers on Q235 Low-carbon Steel Treated by Plasma Electrolytic Borocarburizing. *J Alloy Compd*. 2013, **578**, 162–169.

16. Li X.-M., Han Y. Porous Nanocrystalline Ti(C_xN_{1-x}) Thick Films by Plasma Electrolytic Carbonitriding. *Electroch Commun*. 2006, **8**, 267–272.

17. Aliofkhazraei M., Sabour Roohaghdam A. A Novel Method for Preparing Aluminum Diffusion Coating by Nanocrystalline Plasma Electrolysis. *Electrochem Commun*. 2007, **9**, 2686–2691.

18. Belkin P.N., Ganchar V.I., Davydov A.D., Dikusar A.I., Pasinkovskii E.A. Anodic Heating in Aqueous Solutions of Electrolytes and its Use for Treating Metal Surfaces. *Surf Eng Appl Electrochem.* 1997, (2), 1–15.

19. Taylor R.A., Phelan P.E. Pool Boiling of Nanofluids: Comprehensive Review of Existing Data and Limited New Data. *Int J Heat Mass Transfer*. 2009, **52**(23–24), 5339–5347.

20. Garbarz-Olivier J., Guilpin C. Etude des discharges electriques produites entre l′electrode et la solution lors des effects d′anode et de cathode dans les electrolytes aqueux. *J Chiem Phys.* 1975, **72**(2), 207–214.

21. Belkin P.N., Ganchar V.I., Petrov Yu.N. Conduction of the Vapor Film during Electrolytic Anode Heating. *Sov Phys Dokl.* 1986, **31**, 1001–1004.

22. Shadrin S.Yu., Belkin P.N. Analysis of Models for Calculation of Temperature of Anode Plasma Electrolytic Heating. *Int J Heat Mass Transfer*. 2012, **55**, 179–186.

23. Shiryaeva S.O., Grigor'ev A.I., Morozov V.V. On the Appearance of Ions Near the Charged Surface of an Intensely Evaporating Electrolyte. *Tech Phys*. 2003, **48**(7), 822–828.

24. Landau L.D., and Lifshitz E.M. *Electrodynamics of Continuous Media*. 2 ed., Vol. 8. Pergamon, 1984, P. 33.

25. Belkin P.N., Ganchar V.I. Passage of a Current Through a Vapor-gas Sheath during Anodic Electrolytic Heating. *Surf Eng Appl Electrochem.* 1988, (5), 97–102.

26. Ganchar V.I., Zgardan I.M., Dicusar A.I. Anodic Dissolution of Chromium during Electrolytic Heating. *Surf Eng Appl Electrochem.* 1996, (5), 13–19.

Received 08.04.15
Accepted 15.05.15
Accepted in revised form 11 August 2015

Реферат

В работе рассматриваются причины образования сплошной и устойчивой анодной парогазовой оболочки (ПГО), в которой проводится электролитно-плазменное насыщение (ЭПН) металлов и сплавов легкими элементами (азотом, углеродом, бором). Установлено, что второе критическое напряжение, связанное с переходом от режима прерываний тока к режиму стационарного нагрева, определяется эмиссией анионов из кипящего электролита в оболочку и условиями передачи тепла в системе. Устойчивость поверхности раздела электролит – оболочка обеспечивается выделением энергии в оболочке вследствие прохождения через нее электрического тока. Второе критическое напряжение, способствующее эмиссии анионов, рассчитано на базе модели Гюи–Чампена и апериодической неустойчивости типа Тонкса–Френкеля. Теоретическая зависимость критического напряжения от концентрации электролита подтверждена экспериментально. Влияние концентрации электролита на второе критическое напряжение объясняется эмиссионной способностью электролита. Влияние скорости течения электролита на это напряжения связано с условиями передачи тепла. Необходимо отметить, что эмиссия анионов объясняет влияние состава электролита на изменение массы образца-анода, предельную температуру нагрева (~1000°C) из-за ограничения эмиссионной способности электролита, дискретный характер тока в случае анода с малой поверхностью и высокочастотные импульсы тока.

Ключевые слова: плазменный электролиз, эмиссия анионов, критическое напряжение.